PCCP

Accepted Manuscript

ROYAL SOCIETY OF CHEMISTRY

www.rsc.org/pccp

PCCP

RSCPublishing

ARTICLE

The Soret absorption band of isolated chlorophyll *a* and *b* tagged with quarternary ammonium ions

Cite this: DOI: 10.1039/x0xx00000x

Mark H. Stockett,[a] Lihi Musbat,[b] Christina Kjær,[a] Jørgen Houmøller,[a] Yoni Toker,[b] Angel Rubio,[c,d] Bruce F. Milne*[d,e] and Steen Brøndsted Nielsen*[a]

Received 00th January 2012,
Accepted 00th January 2012

DOI: 10.1039/x0xx00000x

www.rsc.org/

We have performed gas-phase absorption spectroscopy in the Soret-band region of chlorophyll (Chl) *a* and *b* tagged by quarternary ammonium ions together with Time-dependent density functional theory (TD-DFT) calculations. This band is the strongest in the visible region of metalloporphyrins and an important reporter on the microenvironment. The cationic charge tags were tetramethylammonium, tetrabutylammonium, and acetylcholine, and the dominant dissociation channel in all cases was breakage of the complex to give neutral Chl and the charge tag as determined by photoinduced dissociation mass spectroscopy. Two photons were required to induce fragmentation on the time scale of the experiment (microseconds). Action spectra were recorded where the yield of the tag as a function of excitation wavelength was sampled. These spectra are taken to represent the corresponding absorption spectra. In the case of Chl *a* we find that the tag hardly influences the band maximum which for all three tags is at 403 ± 5 nm. A smaller band with maximum at 365 ± 10 nm was also measured for all three complexes. The spectral quality is worse in the case of Chl *b* due to lower ion beam currents; however, there is clear evidence for the absorption being to the red of that of Chl *a* (most intense peak at 409 ± 5 nm) and also a more split band. Our results demonstrate that the change in the Soret-band spectrum when one peripheral substituent (CH_3) is replaced by another (CHO) is an intrinsic effect. First principles TD-DFT calculations agree with our experiments, supporting the intrinsic nature of the difference between Chl *a* and *b* and also displaying minimal spectral changes when different charge tags are employed. The deviations between theory and experiment have allowed us to estimate that the Soret-band absorption maxima *in vacuo* for the neutral Chl *a* and Chl *b* should occur at 405 nm and 413 nm, respectively. Importantly, the Soret bands of the isolated species are significantly blueshifted compared to those of solvated Chl and Chl-proteins. The protein microenvironment is certainly not innocent of perturbing the electronic structure of Chls.

Introduction

Chlorophyll (Chl) *a* and *b* are the light-absorbers of plants and are composed of a porphyrin macrocyle with a divalent magnesium ion in the centre. The ππ* transitions in the macrocycle are responsible for the strong absorption of these molecules which spans most of the visible spectrum except for the green region (which is the reason for the green colour of plants). There are two main absorption bands denoted the Soret and the Q bands, the latter covering the absorption by proteins in the red region while the former is in the blue. The only difference between Chl *a* and Chl *b* is one of the peripheral substituents that in Chl *a* is a formyl group (CHO) and in Chl *b* a methyl group (CH_3). Just this small difference causes the Soret band of Chl *b* to be redshifted compared to that of Chl *a* while the opposite is true for the Q bands.[1,2] Hence by using two different chlorophylls instead of one, plants absorb over a broader region and thereby better take advantage of the solar spectrum.

It is nontrivial to predict the absorption spectra of Chl *a* and *b* and what effect the protein environment has.[2] Axial ligation, nonspecific interactions with nearby amino acid residues, and exciton coupling between two or more Chls can all be expected to contribute to modulation of the absorption.[4] Similarly, solution-phase absorption spectra will display a significant dependence on the solvent used. To disentangle different effects it is desirable (or even necessary) to possess accurate knowledge of the absorption characteristics of isolated Chls *in vacuo*, the simplest of all situations. In our previous work we recorded gas-phase absorption spectra in the Q-band region and found that the isolated molecules displayed significantly blueshifted absorption spectra compared to their protein analogues, by as much as 70 nm.[5] Interestingly, we found the difference between Chl *a* and Chl *b* Q-bands to be an intrinsic effect which does not necessarily involve microenvironmental interactions with the carbonyl group of Chl *b*. The absorption was obtained indirectly from action spectroscopy where the yield of a fragment ion was monitored as a function of excitation wavelength using a mass spectrometer. However, as Chl is a neutral molecule not amenable to conventional mass spectroscopy, we tagged the molecules with quarternary ammonium ions, namely tetramethylammonium ($\mathbf{1}^+$), tetrabutylammonium ($\mathbf{2}^+$), or acetylcholine ($\mathbf{3}^+$). These charge tags have no mobile protons so we know with certainty where the charge is located. Spectra were found to be surprisingly independent of the charge tag which indicated that it was remote from the π electron cloud. Density Functional Theory (DFT) calculations fully supported this idea. While theory also showed very little dependence on the charge tag, the computed vertical excitation energies were systematically blueshifted by 0.11 eV for Chl *a* and on average 0.15 eV for Chl *b* relative to experimental band maxima. This deviation, however, allowed us to calibrate calculated values for bare molecules with no charge tags and obtain best estimates of the lowest-energy Q_y(0-0) band (642 nm for Chl *a* and 626 nm for Chl *b*).

Previous work was also done by Saito *et al.*[6] on deprotonated Chl *a* and Chl *b*; however, the absorption is significantly different to those of the neutral chromophores as the conjugated network is changed upon deprotonation.

Here our focus is on the Soret-band absorption, and we make use of the same charge-tagging method introduced above. In the previous work we could only conclude that the band maximum was below 420 nm, the lower end of the visible output from the optical parametric oscillator (OPO) that was used for the experiments.

Experimental

To produce light below 420 nm with enough intensity for the current experiments, we constructed a new laser module mixing the fundamental output from a Nd:YAG laser (1064 nm) with the visible output from the OPO (to be described elsewhere). Due to technical limitations of this new laser system, our spectra are of lower quality than those in the Q-band region, but are still good enough to make firm conclusions.

Experiments were done with a home-built sector instrument equipped with an electrospray ion source and a tuneable laser system described in detail elsewhere.[7,8] All compounds, Chl *a*, Chl *b*, both from spinach, salts of tetramethylammonium, tetrabutylammonium, and acetylcholine were obtained from Sigma-Aldrich. Methanol solutions of chlorophyll *a* and *b* and the charge tag were made and electrosprayed. All ions were accumulated in an octopole trap that was emptied every 25 ms (40-Hz repetition rate) to produce 10-μs long ion bunches. Acceleration to 50-keV energies was followed by selection of ions of interest according to mass-to-charge ratio by a bending magnet. These were then irradiated by light from a pulsed laser system: The fundamental from a Nd:YAG laser (EKSPLA) was frequency tripled to 355-nm ultraviolet light that was split into a visible photon (420 – 720 tuneable range) and an infrared idler photon in an optical parametric oscillator (OPO). The 1064-nm fundamental was mixed with the visible OPO output in the home-made laser module to produce light in the 301 - 425 nm range. The length of the laser pulses was a few nanoseconds with a 20 Hz firing rate. Hence only every second ion bunch was irradiated which allowed us to obtain the pure photoinduced signal as 'laser on' minus 'laser off'. Fragment ions formed were analysed by a hemispherical electrostatic analyser (ESA) (according to kinetic energy per charge) and counted by a channeltron detector. A LabView program was used to synchronise the laser triggering and the ion trap emptying time. Three different experiments were done: 1) Photoinduced dissociation mass spectroscopy: The ESA was scanned at a fixed laser wavelength. 2) Power dependence: The yield of a fragment ion was monitored as a function of laser power to determine the number of photons required for its formation on the time scale of the experiment (up to 20 microseconds). Neutral density filters were used to attenuate the laser beam. 3) Action spectroscopy: The photo-induced yield of a fragment ion *versus* excitation wavelength was recorded.

Computational details

The geometries of all compounds/complexes were optimised at the DFT level using the gradient-corrected PBE functional[9,10] and the Def2-SVP[11,12] polarised split-valence basis set. The Orca software package was used for all geometry optimisations.[13] Default cut-off criteria for convergence of the self-consistent field and nuclear gradient calculations were employed. Previously it was found that the complexation of acetylcholine cation to Chl did not involve interaction with the Mg^{2+} ion and so this binding mode was again excluded for the present work.

Excitation energies were calculated using time-dependent DFT[14] with the GAMESS-US software (1st October 2010 (R1) release).[15] The range-separated CAM-B3LYP functional[16,17] was selected as this had previously been shown to provide good results for the gas-phase Q-band spectra of Chl *a* and *b* and similar to those obtained with the computationally demanding

equation of motion coupled-cluster level of theory.[18,19] Similarly, the Def2-SVP basis set was selected for these calculations because previous work had shown that it provided results in good agreement with experiment.[19] Several extremely weak excitations with oscillator strengths approaching zero were found lying between the Q and Soret bands, and for this reason it was necessary to include the first 15 excited states of the Chl systems in order to capture the excitations corresponding to the Soret band.

Results and discussion

Experimental results

Photoexcitation of complexes between Chl *a*/*b* and a quaternary ammonium tag led in all cases to separation of the complex. A representative example is shown in Figure 1 for Chl *a* • $\mathbf{1}^+$ where the wavelength of light is 360 nm, and the dominant fragment ion is $\mathbf{1}^+$ (*m/z* 74). Figure 2 shows the production of this fragment ion as a function of laser power. Clearly more than one photon is needed to cause dissociation within the instrumental time for sampling dissociation (up to about 20 microseconds, see ion bunch profile in ESI). A quadratic fit seems to account nicely for the data, which indicates that two photons are required. The data points at maximum laser power were not included as saturation occurred corresponding to photoexcitation of all ions in the interaction volume (a two-photon Poisson fit including saturation fully accounts for all points, see ESI). To obtain action spectra, the photoinduced signal should therefore be divided by the number of photons raised to the power of two.

These action spectra are taken to represent the absorption spectra of the ions. This is valid when the fluorescence is insignificant or the fluorescence quantum yields do not depend on the excitation wavelength. Quantum yields have not been measured for gas-phase molecules but are 0.25 for solvated Chl *a* independent of solvent and excitation wavelength and 0.11 and 0.06 for Chl *b* in ether and methanol solutions, respectively.[20]

Action spectra of Chl *a* • $\mathbf{3}^+$ and Chl *b* • $\mathbf{3}^+$ recorded by sampling the yield of $\mathbf{3}^+$ as a function of wavelength are shown in Figure 3. They were obtained after averaging of six and five scans, respectively, taken with 1-nm steps, and smoothing by 12-point sliding averages (raw spectra are shown in the ESI). The laser beam overlap with the ion beam oscillates slightly due to the finite step size by which we can move the prism in the laser module, which is needed to separate the generated photon from the 1064-nm and visible photon. This means that we have to be cautious in over-interpreting the band shapes. However, both ions reveal absorption below 425 nm, and the major band for Chl *a* is blueshifted relative to that for Chl *b*. Hence the observation in proteins and in solutions that the Soret band of Chl *a* is to the blue of that of Chl *b* is obtained also for the gas-phase complexes. Hence this shift is an intrinsic effect originating from the methyl and formyl ring substituents being different. A similar conclusion was drawn for the Q band that was found to be further to the red for Chl *a* than for Chl *b*.[5] The band maximum is at 404 ± 5 nm for Chl *a* • $\mathbf{3}^+$ while the maximum is at 409 ± 5 nm for Chl *b* • $\mathbf{3}^+$ but with a shoulder at 422 nm. Also a shoulder at about 440 nm was earlier seen for Chl *b*. The Soret band is broad or split (in the case of Chl *b*) which is due to the asymmetry of the Chl molecule and therefore different transition dipoles along the *x*- and *y*-axes of the porphyrin ring as well as vibronic coupling. There is also absorption occurring at wavelengths below 380 nm, with maxima at about 365 nm and 340 nm.

We note that we have tested for reproducibility by repeating the experiment for Chl a • $\mathbf{3}^+$ two months later than the first measurements and also with a lower acceleration voltage of 25 kV (see ESI). At 25-kV acceleration the time for dissociation is on average longer than at 50-kV acceleration but there was no significant difference between the action spectra. Hence we assume that most ions that have absorbed two photons dissociate before reaching the ESA over the whole wavelength region.

The dependence on the charge tag of the absorption by Chl *a* is evident from Figure 4. The band width for Chl *a* • $\mathbf{2}^+$ seems a bit narrower than those of the two others but otherwise the spectra are quite similar The band maxima are at 403 ± 5 nm, 404 ± 5 nm, and 404 ± 5 nm for Chl *a* tagged with $\mathbf{1}^+$, $\mathbf{2}^+$, and $\mathbf{3}^+$. Hence as for the Q-band region, the charge tag plays a minor role for the Soret-band absorption in accordance with its location far away from the π electron cloud and attached to the carbonyl oxygens of the sidechains. A similar conclusion is reached from comparison of Chl *b* • $\mathbf{1}^+$ with Chl *b* • $\mathbf{3}^+$. Band maxima are summarised in Table 1 and compared with values obtained from the theoretical calculations.

In Figure 5 we show the full spectra of Chl *a* • $\mathbf{3}^+$ and Chl *b* • $\mathbf{3}^+$ covering both the Soret-band and Q-band regions, the latter based on previously published spectra[5]. As mentioned before the Soret band is blue-shifted for Chl *a* compared to Chl *b* while the opposite is true for the Q band. It seems that the relative strength between the Soret band and the Q band is higher for Chl *a* than for Chl *b*. However, it should be noticed that spectra were combined based on the overlap in the relatively small region of 420-425 nm where the absorption by Chl *a* is changing rapidly.

Theoretical results and comparison with experimental data

Details of the geometries and binding of the charge tags to the Chl molecules have been given previously and will not be discussed further here.[5]

The TD-CAM-B3LYP calculated excitations energies for the variously tagged Chls along with those of the bare neutral Chl *a* and *b* are shown in Tables 1 and 2. An arbitrary oscillator strength cut-off of 0.1 was used to eliminate unimportant excitations in the regions of interest and improve the clarity of the tabulated data. Details of the electronic transitions and their orbital components contributing to the individual excitations

underlying the bands observed in the experimental spectra are provided in Tables S1 and S2 in the ESI.

For the isolated Chl *a* and *b* it was found that the Soret-band region was composed of three excitations with a separation between the highest and lowest energy excitations of approximately 2 eV. When the charge tags were present, the excitation of intermediate energy was suppressed and no longer contributed significantly to the band; however, the other two excitations remained at more or less the same energy as in the bare-chromophore cases.

Regardless of the nature (or absence) of the charge tag a redshift of around 0.1 to 0.2 eV was noted in the Soret-band excitations of Chl *b* relative to those of Chl *a*, in good agreement with experiment (see Figs. 3-5).

The geometrical means of the contributing calculated excitations were used for comparison with the Soret-band maxima recorded experimentally (Table 1). This permitted the calculation of the average deviations between theory and experiment which were found to be +0.44 eV for Chl *a* and +0.29 eV for Chl *b*. By subtracting these figures from the Soret-band averages calculated for the bare neutral Chls it was possible to estimate values for the isolated chlorophyll Soret band *in vacuo* of 3.06 eV (405 nm) for Chl *a* and 3.00 eV (413 nm) for Chl *b*.

The weaker, higher-energy band observed in the experimental spectra was also reproduced well by the TD-CAM-B3LYP calculations. Experimentally this band was observed to lie approximately 0.3 eV higher in energy than the Soret band at 365 ± 10 nm whilst in the calculated spectra this blueshift was around 0.5 eV. The relative intensities of the Soret band and this minor band were also well reproduced with the minor band's excitations possessing oscillator strengths around one quarter of those of the Soret-band excitations (compare tabulated values in Table 2 with spectra in Figures 3 and 4).

Comparison with solvated-Chl and pigment-protein spectra

In diethyl ether Chl *a* has band maxima at 428 nm, 409 nm, 379 nm, and 326 nm while the lowest energy maximum is at 418 nm in methanol.[19] Chl *b* has band maxima at 453 nm and 429 nm in diethyl ether. Hence solvation causes significant redshifts of the Soret band for both Chl *a* and Chl *b*. As the resolution of our gas-phase spectra is poor, we can only say that the shift of the most intense peak of the Soret band is <23 nm for Chl *a* and <30 nm for Chl *b*.

In leaves all Chl pigment molecules are linked to proteins and display different absorption[21]: Light-harvesting Chl *a*, *b*-protein complexes have band maxima at 437 nm and 472 nm and the Chl *a* of photosystem II reaction centers at 437 nm. Hence the nearby protein environment causes larger shifts than those upon solvation. The shifts are likely due to either axial ligation or exciton coupling or a combination hereof. Heimdal *et al.*[4] calculated shifts due to axial ligation between 3 and 35 nm, the largest effect being for negatively charged ligands. More work to decipher the effect of axial ligation on the absorption by the gas-phase complexes would be needed to address this issue in more detail and to verify the calculations.

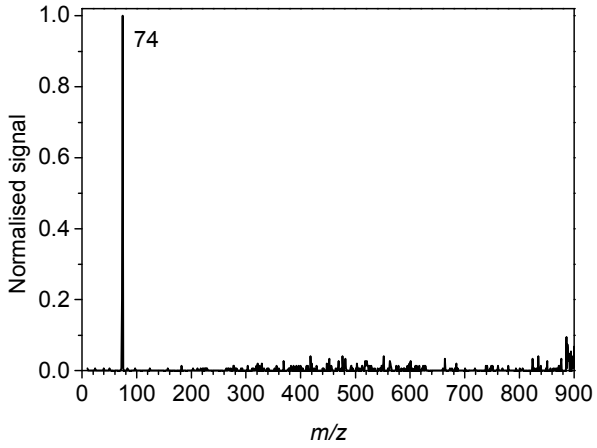

Figure 1. Photoinduced dissociation (PID) mass spectrum of Chl *a* • $\mathbf{1}^+$. λ = 360 nm. The dominant fragment ion is the charge tag with mass 74.

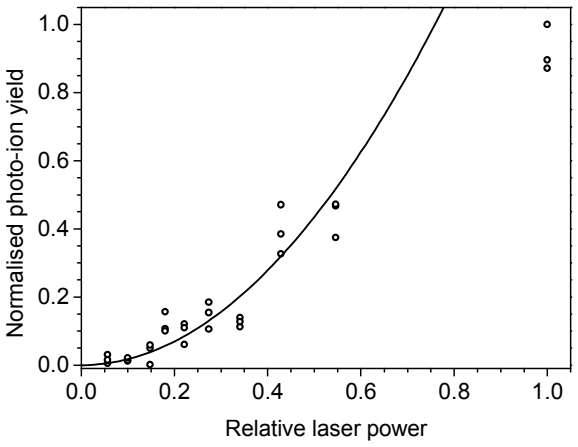

Figure 2. Power dependence for the formation of $\mathbf{1}^+$ from Chl *a* • $\mathbf{1}^+$. λ = 360 nm. An ax^2 function was fit to the data neglecting the highest laser power where saturation occurred.

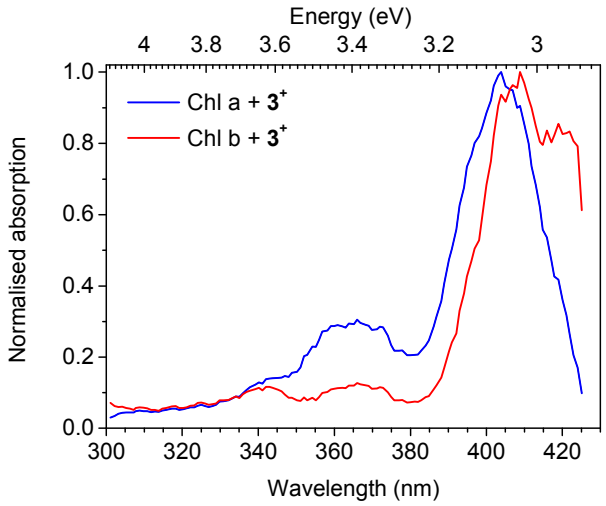

Figure 3. Action spectra of Chl *a* • $\mathbf{3}^+$ and Chl *b* • $\mathbf{3}^+$. These are taken to represent the absorption by the ion-molecule complexes. The maximum of the band is set to 1.

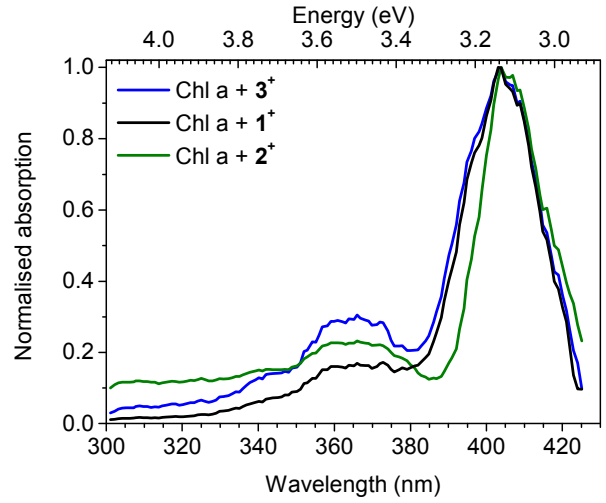

Figure 4. Action spectra of Chl *a* with the three different charge tags. The spectra are taken to represent the absorption by the ion-molecule complexes.

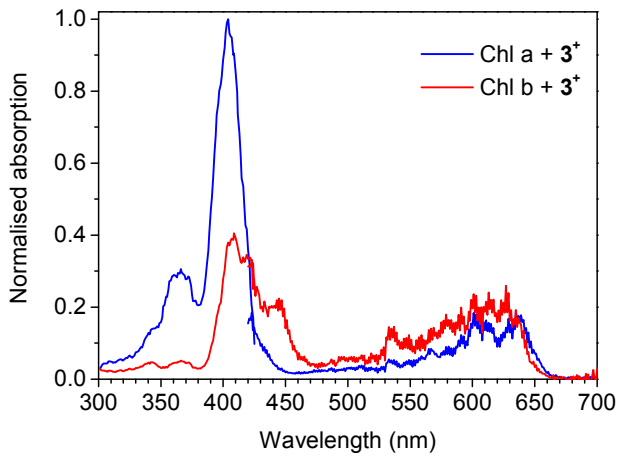

Figure 5. Action spectra of Chl *a* • $\mathbf{3}^+$ and Chl *b* • $\mathbf{3}^+$ in the Soret and Q-band regions. The total spectra are made by combining spectra taken from 300 nm to 425 nm (present work) with spectra from 420 nm to 700 nm (previous work)[5].

Table 1. Summary of experimental band maxima and vertical transition energies (in eV) for the Soret band.[a]

	$\mathbf{1}^+$	$\mathbf{2}^+$	$\mathbf{3}^+$	No tag	Diethyl-ether
Exp. Chl *a*	3.08 (403)	3.07 (404)	3.07 (404)	3.06 (405)[b]	2.90 (428)
Theory Chl *a*	3.54 (350)	3.51 (354)	3.48 (356)	3.47 (358)	
Exp. Chl *b*	3.03 (409)		3.03 (409)	/ 3.00 (413)[b]	2.73 (453)
Theory Chl *b*	3.34 (371)	3.32 (374)	3.29 (377)	3.28 (378)	

[a] Corresponding absorption wavelengths are provided in parenthesis (in nm).
[b] Estimated values based on deviation between theory and experiment for tagged Chls.

Table 2. TD-CAM-B3LYP/Def2-SVP transition energies contributing to the Soret band and secondary minor peak. Values in eV with oscillator strengths in parentheses.

	1^+	2^+	3^+	No tag
Chl *a*				
Soret	3.42 (0.91)	3.38 (0.87)	3.36 (0.78)	3.34 (0.65)
	3.67 (0.81)	3.64 (0.79)	3.60 (0.73)	3.45 (0.41)
				3.61 (0.90)
Minor	3.99 (0.11)	4.07 (0.24)	3.92 (0.29)	4.00 (0.17)
peak	4.07 (0.25)		4.08 (0.23)	
			4.14 (0.15)	
			4.17 (0.19)	
Chl *b*				
Soret	3.25 (1.00)	3.23 (0.939)	3.20 (0.86)	3.16 (0.68)
	3.43 (0.72)	3.41 (0.747)	3.38 (0.75)	3.32 (0.83)
				3.37 (0.39)
Minor	4.02 (0.11)	4.14 (0.297)	3.93 (0.20)	4.21 (0.12)
peak	4.13 (0.28)		4.11 (0.13)	
			4.13 (0.23)	
			4.14 (0.15)	

Conclusions

We have provided a detailed experimental and theoretical study of the Soret absorption band of isolated chlorophyll *a* and *b* in the presence of quarternary ammonium ions (charge tags). Good agreement between experimental and theoretical (TD-DFT) data on the ion-molecule complexes allowed us to calibrate calculated values for bare Chl *a* and Chl *b*; our best estimates of the Soret-band maxima *in vacuo* are 405 nm and 413 nm. The absorption by Chl *a* is blueshifted relative to Chl *b* as also seen for solvated Chl *a* and *b* and when the two pigments are situated in proteins. Our work shows this to be an intrinsic effect that does not necessarily involve microenvironmental perturbations with the formyl group of Chl *b*. Still the gas-phase absorption spectra are significantly blueshifted compared to protein spectra, which emphasises the strong effect of the microenvironment on the overall transition energies. Particularly axial ligation to the magnesium centre is expected to play a role, which is to be explored more in the future.

Acknowledgements

SBN and MHS acknowledge Lundbeckfonden and Villumfonden for support. BFM thanks the Donostia International Physics centre and the Centre de Física de Materiales, University of the Basque Country for financial support. BFM also thanks the Laboratory for Advanced Computing of the University of Coimbra, Portugal for the provision of computer resources, technical support and assistance. AR acknowledges financial support from the European Research Council Advanced Grant DYNamo (ERC-2010- AdG-267374), Spanish Grant (FIS2013-46159-C3-1-P), Grupos Consolidados UPV/EHU del Gobierno Vasco (IT578-13) and European Community FP7 project CRONOS (Grant number 280879-2) and COST Actions CM1204 (XLIC) and MP1306 (EUSpec). LM and YT acknowledge Cost Action CM1204 (XLIC) for support (ECOST-STSM-CM1204-301114-047659).

Notes and references

[a] Department of Physics and Astronomy, Aarhus University, Ny Munkegade 120, DK-8000 Aarhus C, Denmark. E-mail: sbn@phys.au.dk
[b] Institute of Nanotechnology and Advanced Materials, Bar-Ilan University, Ramat-Gan 290002, Israel.
[c] Max Planck Institute for the Structure and Dynamics of Mattere and Center for Free-Electron Laser Science, Luruper Chaussee 149, 22761 Hamburg, Germany.
[d] Nano-Bio Spectroscopy Group and ETSF, Dpto. Fisica de Materiales, Universidad del País Vasco, CFM CSIC-UPV/EHU-MPC & DIPC, 20018 San Sebastián, Spain.
[e] Centre for Computational Physics, Department of Physics, University of Coimbra, Rua Larga, 3004-516 Coimbra, Portugal. E-mail: bruce@teor.fis.uc.pt.

Electronic Supplementary Information (ESI) available: [Ion bunch profiles; action spectra at 25-kV and 50-kV ion kinetic energies; Orbital contributions to calculated TD-CAM-B3LYP/Def2-SVP excitations]. See DOI: 10.1039/b000000x/

1 J. Gross, Pigments in vegetables: chlorophylls and carotenoids, Springer, New York, 1991.
2 G.C. Papageorgiou, "Fluorescence of Photosynthetic Pigments in Vitro and in Vivo" in G.C. Papageorgiou and Govindjee (Eds.), Advances in Photosynthesis and Respiration, Volume 19, Chlorophyll a Fluorescence. A Signature of Photosynthesis. Springer, Dordrecht 2004.
3 J. Linnanto and J. Korppi-Tommola, *Phys. Chem. Chem. Phys.*, 2006, **8**, 663.
4 J. Heimdal, K.P. Jensen and A. Devarajan and U. Ryde, *J. Biol. Inorg. Chem.*, 2007, **12**, 49.
5 B.F. Milne, Y. Toker, A. Rubio and S. Brøndsted Nielsen, *Angew. Chem. Int. Ed.*, 2015, **54**, 2170.
6 M. Saito, T. Tanabe, K. Noda and M. Lintuluoto, *Phys. Rev. A*, 2013, **87**, 033403.
7 K. Støchkel, B.F. Milne and S. Brøndsted Nielsen, *J. Phys. Chem. A*, 2011, **115**, 2155.
8 J.A. Wyer and S. Brøndsted Nielsen, *Angew. Chem. Int. Ed.*, 2012, **51**, 10256.
9 J. Perdew, M. Ernzerhof and K. Burke, *J. Chem. Phys.*, 1996, **105**, 9982.
10 J.P. Perdew, K. Burke and M. Ernzerhof, *Phys. Rev. Lett.* 1996, **77**, 3865; J.P. Perdew, K. Burke and M. Ernzerhof, *Phys. Rev. Lett.*, 1997, **78**, 1396.
11 A. Schäfer, H. Horn and R. Ahlrichs, *J. Chem. Phys.*, 1992, **97**, 2571.
12 F. Weigend and R. Ahlrichs, *Phys. Chem. Chem. Phys.*, 2005, **7**, 3297.
13 F. Neese, *Comput. Mol. Sci.*, 2012, **2**, 73.
14 E. Runge and E.K.U. Gross, *Phys. Rev. Lett.*, 1984, **52**, 997
15 M.W. Schmidt, K.K. Baldridge, J.A. Boatz, S.T. Elbert, M.S. Gordon, J.H. Jensen, S. Koseki, N. Matsunaga, K.A. Nguyen, S.J. Su, T.L. Windus, M. Dupuis and J.A. Montgomery, *J. Comput. Chem.*, 1993, **14**, 1347.
16 M.J.G. Peach, P. Benfield, T. Helgaker and D.J. Tozer, *J. Chem. Phys.*, 2008, **128**, 044118.

17 M.J.G. Peach, C.R.L. Sueur, K. Ruud, M. Guillaume and D.J. Tozer, *Phys. Chem. Chem. Phys.*, 2009, **11**, 4465.
18 K. Støchkel, C.N. Hansen, J. Houmøller, L.M. Nielsen, K. Anggara, M. Linares, P. Norman, F. Nogueira, O.V. Maltsev, L. Hintermann, S. Nielsen Brøndsted, P. Naumov and B.F. Milne, *J. Am. Chem. Soc.*, 2013, **135**, 6485.
19 H. Du, R.-C.A. Fuh, J. Li, L.A. Corkan and J.S. Lindsey, *Photochem. Photobiol.*, 1998, **68**, 141; J.M. Dixon, M. Taniguchi and J.S. Lindsey, *Photochem. Photobiol.*, 2005, **81**, 212.
20 L.S. Forster and R. Livingston, *J. Chem. Phys.*, 1952, **20**, 1315.
21 J.R. Evans and J.M. Anderson, *Biochimica et Biophysica Acta*, 1987, **892**, 75.